01 Dec 1973

Properties Of Microwave Cavities Containing Magnetic Resonant Samples

Kathy A. Rages

Robert E. Sawyer

Edward Boyd Hale
Missouri University of Science and Technology, ehale@mst.edu

Recommended Citation

K. A. Rages et al., "Properties Of Microwave Cavities Containing Magnetic Resonant Samples," *Review of Scientific Instruments*, vol. 44, no. 7, pp. 830 - 834, American Institute of Physics, Dec 1973.
The definitive version is available at https://doi.org/10.1063/1.1686258

RESEARCH ARTICLE | NOVEMBER 06 2003

Properties of Microwave Cavities Containing Magnetic Resonant Samples

Kathy A. Rages; Robert E. Sawyer; Edward B. Hale

Rev Sci Instrum 44, 830–834 (1973)
https://doi.org/10.1063/1.1686258

Properties of Microwave Cavities Containing Magnetic Resonant Samples*

Kathy A. Rages† and Robert E. Sawyer‡
Physics Department, University of Missouri—Rolla, Rolla, Missouri 65401

Edward B. Hale
Physics Department and Materials Research Center, University of Missouri—Rolla, Rolla, Missouri 65401
(Received 27 November 1972; and in final form, 23 March 1973)

Properties of TE_{011} cylindrical, microwave cavities containing cylindrical samples of various radii and dielectric constants are calculated. The properties considered are the resonant frequency, quality factor (Q), relevant magnetic filling factor for spin transitions (η), and a signal sensitivity factor ($Q\eta$) for a lossless sample. Sample sizes range from zero radius to full cavity radius with some experimental data on less than full length samples. The choice of dielectric constants ranges from one to sixteen. The data are presented in dimensionless form since they will be of use to other ESR experimentalists. It is shown that use of large samples is undesirable even if they are lossless. Furthermore, elongated cavities (D/L ratios less than one) are to be preferred over shortened cavities.

INTRODUCTION

Measurements are often made to determine the spin magnetic resonance parameters of a dielectric sample inside a microwave cavity. In these measurements, the cavity is placed in a large, homogeneous dc magnetic field, $\mathbf{H}_0$, and microwave excitation is introduced into the cavity. The component of the microwave magnetic field perpendicular to $\mathbf{H}_0$ induces the spin transitions of interest. The cavity is used to enhance the detection of these transitions. This is accomplished by choosing the microwave frequency, ω, to be a tuned, resonant frequency of the cavity with sample and by arranging the cavity and sample configuration to yield a large $Q\eta$ factor, where Q is the quality factor and η is the relevant magnetic filling factor for the sample in the cavity. (The signal sensitivity is proportional to the $Q\eta$ product.[1]) The purpose of this paper is to examine these three parameters (ω, Q, and η) for very common cavity and sample configurations.

The configuration considered is shown in Fig. 1. The cylindrical sample of radius R_1, length L, and dielectric constant κ_1 is surrounded by a medium of dielectric constant, κ_2, and is coaxial with a metal cavity of radius R_2 and length L. The field $\mathbf{H}_0$ is applied in the r–ϕ plane. For the TE_{011} resonant mode the microwave field, H_z, is maximum at $r=0$ and is the major perpendicular field component. This mode is used in many of the available commercial cavities by such manufacturers as Varian, JEOLCO, Bruker Scientific, and Ventron.

Our calculations have been performed in such a manner that they should be reasonably valid or easily adapted to many of the commercial TE_{011} cylindrical cavities. The calculations are for a fixed cavity size (i.e., constant L and R_2), which is vacuum or air filled outside the sample (i.e., $\kappa_2=1$). The sample size and dielectric constant (i.e., R_1 and κ_2) are treated as variables. The sample is assumed lossless, which is certainly not unrealistic for small R_1 since the only nonzero microwave electric field component is zero along the z-axis. In addition, the sample is assumed to be linear, isotropic, and nonferromagnetic. In general, the relevant properties ω, Q, and η are normalized or referenced to the empty ($R_1=0$) cavity values, which are subscripted with a zero. This dimensionless form of normalization was used because the results apply to a rather wide range of sample and cavity configurations. In addition, a wide range of sample dielectric constant ($\kappa=1$ to 16) was chosen so that ESR investigators working with gases, alkali halides, oxides, semiconductors at low temperatures, or other samples having reasonably small loss would find the results useful.

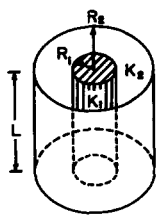

FIG. 1. Sample and cavity configuration. The cylindrical cavity inner dimensions are radius R_2 and length L. The full length sample is a cylinder of radius R_1 and dielectric constant κ_1.

A previous publication[2] considered small lossy samples in a TE_{011} mode cavity. In the present paper perturbation methods are not used, small and large samples with a wide range of dielectric constants are treated, and emphasis is on graphical results, which we believe other investigators can analyze to fit their needs.

I. BASIC DEFINITIONS AND FORMULATIONS

A. Fields and Boundary Conditions

The microwave fields at frequency ω in a TE_{mnp} mode with $m=0$ and configuration as in Fig. 1 are, in mks units,

$$\begin{aligned} B_z &= A_1 J_0(\gamma_1 r)\sin(p\pi z/L)e^{-i\omega t} \\ B_r &= (p\pi/\gamma_1 L)A_1 J_0'(\gamma_1 r)\cos(p\pi z/L)e^{-i\omega t} \\ E_\phi &= (i\omega/\gamma_1)A_1 J_0'(\gamma_1 r)\sin(p\pi z/L)e^{-i\omega t} \end{aligned} \quad (1)$$

inside the sample, and

$$\begin{aligned} B_z &= [A_2 J_0(\gamma_2 r)+B_2 N_0(\gamma_2 r)]\sin(p\pi z/L)e^{-i\omega t} \\ B_r &= (p\pi/\gamma_2 L)[A_2 J_0'(\gamma_2 r)+B_2 N_0'(\gamma_2 r)]\cos(p\pi z/L)e^{-i\omega t} \\ E_\phi &= (i\omega/\gamma_2)[A_2 J_0'(\gamma_2 r)+B_2 N_0'(\gamma_2 r)]\sin(p\pi z/L)e^{-i\omega t} \end{aligned} \quad (2)$$

outside the sample, and $E_z=E_r=B_\phi=0$ everywhere.[3] In the above, J_0 and N_0 are the zero-order Bessel functions and

$$\gamma_i^2 \equiv \kappa_i \epsilon_0 \mu_0 \omega^2 - (p^2\pi^2/L^2), \quad \text{for } i=1, \text{ or } 2. \quad (3)$$

The constant A_1 is determined by the excitation field. The constants to be determined from the boundary conditions are then A_2, B_2, and the frequency ω.

The boundary conditions required that $\mathbf{E}_{\tan}$ and $\mathbf{B}_{\text{normal}}$ are zero at the cavity surfaces. These conditions at the cavity top and bottom determine the sine and cosine dependence as given in Eqs. (1) and (2). At R_2, the E_ϕ equation yields

$$A_2 J_0'(\gamma_2 R_2)+B_2 N_0'(\gamma_2 R_2)=0. \tag{4}$$

The continuity of $\mathbf{E}_{\tan}$, $\mathbf{H}_{\tan}$, $\mathbf{B}_{\text{normal}}$, and $\mathbf{D}_{\text{normal}}$ at the R_1 interface yield

$$(1/\gamma_1)A_1 J_0'(\gamma_1 R_1)=(1/\gamma_2)[A_2 J_0'(\gamma_2 R_1)+B_2 N_0'(\gamma_2 R_1)] \tag{5}$$

and

$$A_1 J_0(\gamma_1 R_1)=A_2 J_0(\gamma_2 R_1)+B_2 N_0(\gamma_2 R_1). \tag{6}$$

B. Resonant Frequencies

The latter three boundary conditions [Eqs. (4)–(6)] can be used to determine ω if they are regarded as three homogeneous equations in the variables A_1, A_2, and B_2. For nontrivial solutions, the vanishing determinant requirement yields

$$F(\omega)\equiv\begin{vmatrix} (\gamma_2/\gamma_1)J_0'(\gamma_1 R_1) & J_0'(\gamma_2 R_1) & N_0'(\gamma_2 R_1) \\ J_0(\gamma_1 R_1) & J_0(\gamma_2 R_1) & N_0(\gamma_2 R_1) \\ 0 & J_0'(\gamma_2 R_2) & N_0'(\gamma_2 R_2) \end{vmatrix}=0. \tag{7}$$

The solutions to this equation are determined to about five or six significant figures using Newton's method in our computer program. The various roots $\omega=\omega_{np}$ are the possible TE_{0np} resonance frequencies.

C. Quality Factor

If losses in the sample are neglected, the quality factor is[1]

$$Q=\frac{2}{\delta}\frac{\int_{V_c} H^2 dV}{\int_{S_c} H^2 dS}, \tag{8}$$

where $\delta(\propto\omega^{-\frac{1}{2}})$ is the classical skin depth of the metal wall material. Calculations yield

$$Q=\frac{2\left[(p^2\pi^2/L^2)\int_0^{R_2} dr\, rR_r(r)+\int_0^{R_2} dr\, rR_z(r)\right]}{\delta\left[R_2R_z(R_2)+(4/L)(p^2\pi^2/L^2)\int_0^{R_2} dr\, rR_r(r)\right]}, \tag{9}$$

where

$$R_r(r)\equiv(1/\gamma_1^2)[A_1 J_0'(\gamma_1 r)]^2, \quad \text{if } r\le R_1$$

or (10)

$$R_r(r)\equiv(1/\gamma_2^2)[A_2 J_0'(\gamma_2 r)+B_2 N_0'(\gamma_2 r)]^2, \quad \text{if } r\ge R_1$$

and

$$R_z(r)\equiv[A_1 J_0(\gamma_2 r)]^2, \quad \text{if } r\le R_1$$

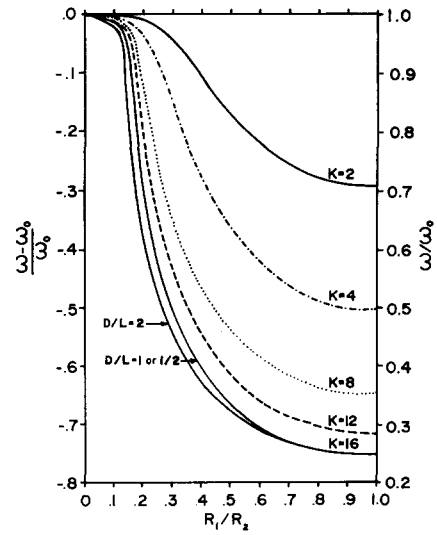

FIG. 2. Normalized resonant frequency shifts for various samples. The frequency shift for $\kappa=16$, and $D/L=2$ is also shown for comparison. Lowering D/L to $\frac{1}{2}$ results in points which are essentially the same as those for $D/L=1$.

or (11)

$$R_z(r)\equiv[A_2 J_0(\gamma_2 r)+B_2 N_0(\gamma_2 r)]^2, \quad \text{if } r\ge R_1.$$

The first term in the denominator is the side wall contribution and the second term is the top and bottom contribution. All radial integrals have been computed by Simpson's method.

D. Filling Factor

The relevant magnetic filling factor is[4]

$$\eta\equiv\frac{\int_{V_s} H^2\sin^2\theta\, dV}{\int_{V_c} H^2\, dV}, \tag{13}$$

where θ is the angle between $\mathbf{H}_0$ and the microwave field $\mathbf{H}(\mathbf{r})$. The numerator integral is over the excitation (i.e., perpendicular) component of the microwave field as required. Calculations yield

$$\eta=\frac{\left[\int_0^{R_1} dr\, rR_z(r)+\frac{1}{2}(p^2\pi^2/L^2)\int_0^{R_1} dr\, rR_r(r)\right]}{\left[\int_0^{R_2} dr\, rR_z(r)+(p^2\pi^2/L^2)\int_0^{R_2} dr\, rR_r(r)\right]}. \tag{13}$$

II. THEORETICAL RESULTS

A. Calculations

The results of the resonant frequency calculations are shown in Fig. 2. The results depend on cavity not through the value of D or L but only via the D/L ratio as might be expected from geometrical scaling arguments. For most of the calculations a D/L ratio of one was chosen, since many commercial cavities have this D/L value. The results for $R_1/R_2=0$ and $R_1/R_2=1$ are independent of the

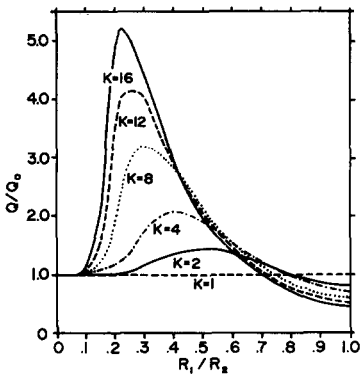

FIG. 3. Normalized quality factors for various samples in a cavity with $D/L=1$.

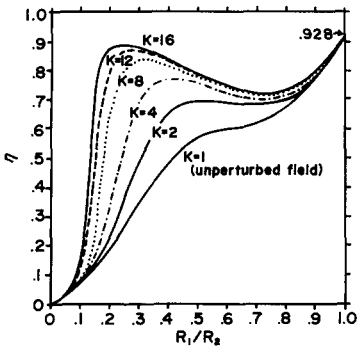

FIG. 5. Magnetic filling factors for various samples. For samples with a high dielectric constant, large η values occur for rather small R_1 values.

D/L ratio. The influence of the D/L ratio is shown for a $\kappa=16$ sample. The values for $R_1=R_2$ agree with the well-known result that[3]

$$\kappa_1(fD)^2=(cx_{01}/\pi)^2+(c\rho/2)^2(D/L)^2, \qquad (14)$$

where c is the velocity of light and $x_{01}=3.83$ is the first root of the first derivative of the zeroth order Bessel function. Thus the $R_1/R_2=1$ results scale as $(\kappa_1)^{\frac{1}{2}}$.

Figure 3 shows the quality factor dependence on R_1 and κ_1. The Q peaks at a value greater than one in all samples with a Q enhancement exceeding five for a material with a dielectric constant of about sixteen. Thus if a high Q cavity is desired for use as a reference cavity or for some other reason, it is clearly advantageous to partially fill it with a high dielectric lossless sample. Note that Q/Q_0 becomes less than one at large R_1 values because the skin depth depends on the resonant frequency [see Eq. (8)]. As in Fig. 2 the curves shown are for $D/L=1$ and depend only on the choice of this ratio. Figure 4 shows the influence of the D/L ratio for $\kappa=16$. Note the enhanced Q values for elongated ($D/L<1$) cavities. The results were calculated at a fixed frequency 9.5 GHz, rather than fixed D for reasons discussed in Sec. II B.

The magnetic filling factor is shown in Fig. 5. The filling factor has a value of 0.928 for all κ when $R_1=R_2$. (The value is less than one because the components of the microwave magnetic field parallel to the dc magnetic field do not contribute to transitions between different spin states.) This filled cavity value can also be obtained directly from Eq. (13) without the use of a computer.

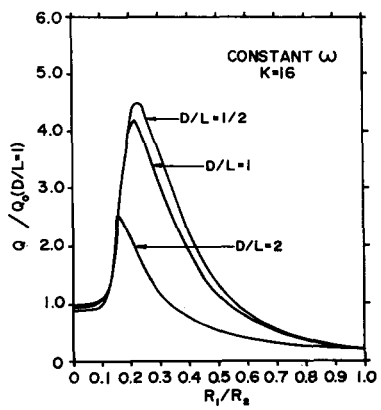

FIG. 4. Effect on Q caused by varying D/L for $\kappa=16$ samples. As D/L increases the maximum Q enhancement decreases, as does the value of R_1/R_2 at which this maximum occurs. The y-axis is normalized to the optimum empty cavity Q_0 value which occurs when $D/L=1$. The results show the advantage of elongated ($D/L<1$) cavities. The results are for a constant frequency as discussed in the text.

The curves shown are for $D/L=1$ and depend only on this ratio. Figure 6 shows the influence of the D/L ratio for $\kappa=16$ samples at a fixed frequency of 9.5 GHz. Note the enhanced η values for elongated cavities.

In Fig. 7 the $Q\eta$ product factor is shown. This factor is proportional to the sensitivity of the spectrometer for a lossless sample.[4] For a material with a fixed dielectric constant, there is an optimum sample size corresponding to the radius at the peak in the appropriate κ curve. A larger size sample would yield a smaller signal.

The $Q\eta$ product factor dependence on D/L is shown in Fig. 8 for a $\kappa=16$ sample. The results are for a fixed resonant frequency and show the important signal enhancement obtainable with elongated cavities.

B. Analysis

The peaks in the various sensitivity curves (Fig. 7) are of prime importance for optimum cavity design. They are produced by the corresponding peaks in the quality factor curves (Fig. 3), but are more pronounced because of the filling factor results (Fig. 5). The peaks in the quality factor curves occur because the appropriate solutions to Maxwell's equations tend to concentrate the fields in the sample rather than outside it. Thus the fields over most of the cavity walls are reduced which reduces the losses in the cavity walls. This reduces the denominator of Eq. (8) and causes an enhancement in Q.

It often occurs that the sample radius is chosen such that the empty cavity resonant frequency is not greatly perturbed. Figure 2 shows that this corresponds to $R_1/R_2\lesssim 0.15$. But, it is clear from Fig. 7 that a sensitivity enhancement of from one to two orders of magnitude can be obtained by simply doubling the sample radius so that

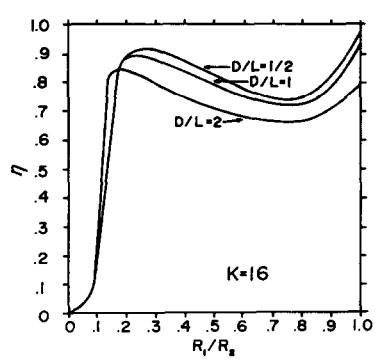

FIG. 6. Effect on η caused by varying D/L for $\kappa=16$ samples. The effects on the peak in η are similar to those on the maximum Q enhancements. The results show the advantages of elongated cavities. Note that the filled cavity η increases with decreasing D/L due to the relative increase in H_z over H_T.

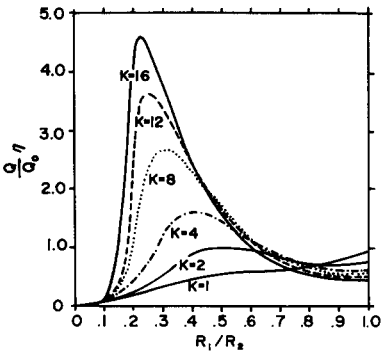

FIG. 7. Product factors for various samples in a $D/L=1$ cavity. This product factor is important for signal detection sensitivity in magnetic resonance experiments.

R_1/R_2 is about one-quarter or one-third. However, further doubling of the sample radius such that $R_1/R_2>\frac{1}{2}$ results in loss of sensitivity and this range of R_1/R_2 values should be avoided.

The $Q\eta$ product factor dependence on D/L is shown in Fig. 8. This dependence is most strongly influenced by the quality factor results (Fig. 4), with the filling factor results (Fig. 6) constructively reinforcing the Q results for most samples. This reinforcement is not accidental since an improvement in sample filling implies a larger energy storage and a reduction in microwave field strength on the cavity surface, i.e., an increased numerator and decreased denominator in Eq. (8). For an *empty* cavity, calculations[3] show that the optimum Q occurs when $D/L=1$. When the cavity contains a sample, the present calculations clearly show that a $D/L=1$ cavity is not an optimum design for the sensitivity factor, the cavity Q, or the sample filling factor. The real importance of these results is that a shortened ($D/L>1$) cavity is to be avoided; an elongated cavity normally yields a small sensitivity enhancement. Qualitatively, this can be understood by noting that the sample expands the effective electrical radial dimension of the cavity. Thus the diameter of the cavity must be reduced to maintain the optimum electrical D/L ratio.

Of practical importance is how to use our results to design cavities for ESR experiments. The following method is suggested. Use Fig. 7 to estimate the R_1/R_2 ratio for optimum sensitivity for the κ of the sample, e.g., for $\kappa=16$, $R_1/R_2\approx\frac{1}{4}$. Using this result, estimate the $(\omega-\omega_0)/\omega_0$ ratio from Fig. 2. Since ω is experimentally restricted to a rather small range by the spectrometer and klystron frequency,

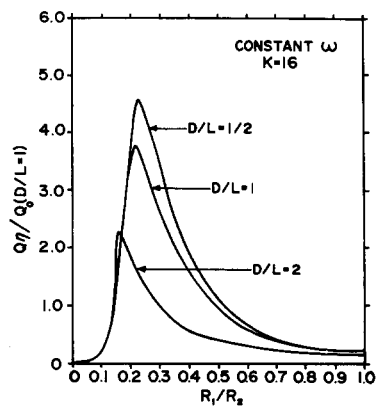

FIG. 8. Product factors for various D/L ratios for a $\kappa=16$ sample. Sensitivity increases with decreasing D/L ratios. Normalization and frequency conditions as in Fig. 4. The results show the advantage of elongated cavities over shortened cavities.

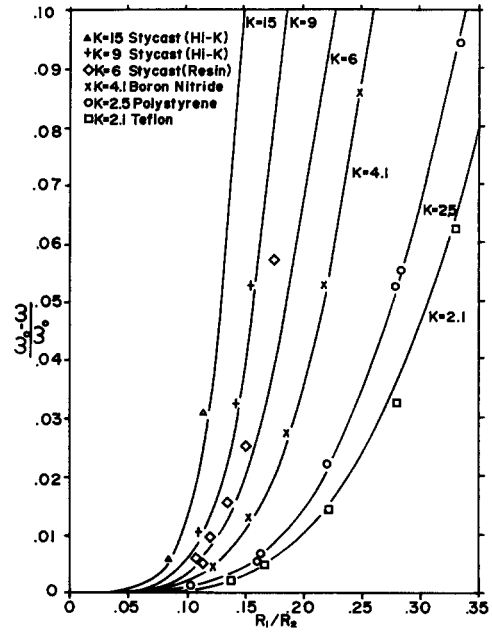

FIG. 9. Experimental normalized frequency shifts for various samples in a $D=L=4.07$ cm cavity. Experimental data points shown by symbols. Solid lines are calculated results from the appropriate solution to Eq. (7).

the above estimate made using Fig. 2, determines ω_0. The diameter of the cavity can then be approximated by the elongated, empty cavity result of Eq. (14). Namely,

$$D=(2cx_{01}/\omega_0), \tag{15}$$

where the approximation of a small D/L ratio has been made. The sample radius is now determined since R_1/R_2 and D are known. Finally, L is chosen to be larger than D so that a near optimum $Q\eta$ factor results (see Fig. 8). Since Fig. 8, or Fig. 4, will normally be used after a choice of ω is made, results presented in these figures are for constant frequency. Results presented in Figs. 3 or 7 are not at constant frequency since they will normally not be used with such a constraint. Note, however, that for any chosen point of the curves in these figures, the frequency can also be chosen to have any value allowable for the TE_{011} mode. (The results presented in Fig. 5 are independent of frequency.)

From a practical point of view, an elongated cavity is usually desirable since a reduced D permits use of a smaller magnet gap and/or greater flexibility in Dewar design.

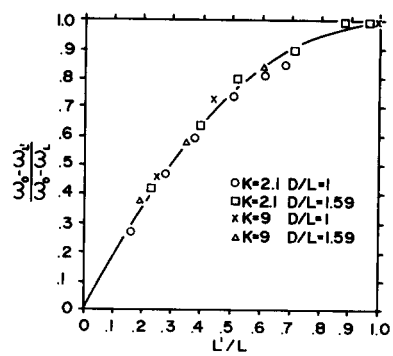

FIG. 10. Experimental resonant frequency shifts for samples of less than full length. Results are normalized to the frequency shifts of the corresponding full length samples.

Often L will be limited either by the sample sizes available or by the magnet, which must not inhomogeneously broaden the ESR lines.

There are several reasons why the above design method may not always be the one used. For example, a small sample may require a design method based on a predetermined R_1 value, or D may be experimentally limited by Dewar size or machining limitations, or a lossy sample may change the $Q\eta$ optimum value from that shown in Fig. 7. (In this latter case, the effects of small, lossy samples can be approximated with the results of Haniotis and Gunthard[2] and should be combined with the present results to obtain a true Q and $Q\eta$ product. Hyde[5] has also considered effects due to lossy samples.) But even in all these cases, the data presented here should still be usable for optimum design.

III. EXPERIMENTAL RESULTS

Experimental verification of the resonance frequency shifts have been obtained. The cavity used was made from copper and had a $D=L=4.07$ cm. Samples used were made from Teflon ($\kappa=2.1$), polystyrene ($\kappa=2.5$), boron nitride ($\kappa=4.1$), and several kinds of Stycast.[6] Measurements were made over the tuning range of a Varian model X-13 reflex kystron.

The experimental results obtained are shown in Fig. 9 by the various symbols. The solid curves are the theoretical predictions. Agreement is verified to within experimental uncertainties. In fact, the dielectric constant for a material can be reasonably estimated by plotting data points on the figure. For example, originally we believed that boron nitride had $\kappa=5$ (see Ref. 7). However, when the data were plotted it appeared that $\kappa=4$. A more detailed literature search determined that $\kappa=4.1$ (see Ref. 8). Our data also seem to indicate that our self-cured samples made from Stycast 36 DK resin have a κ nearer seven rather than the suggested manufacturer's value of six.[9] In addition to the results plotted in Fig. 9, data points in good agreement with theory were also obtained for Teflon samples out to $R_1/R_2=0.8$.

Experiments with samples less than full length have also been performed. Figure 10 shows the effect on the resonance frequency caused by a sample of length L' in a cavity of length L. Data were taken for two different dielectric materials in two different X-band cavities. The frequency shifts were normalized to the full length sample shifted values so that generalized results could be shown on the same graph. In Fig. 10 the solid line is not a theoretical curve; it is merely an approximate best fit to the experimental points. It is probable that there are slight differences in the actual relationships between length and resonance frequency for the cases shown. However, these differences are within the experimental error limits.

The influence of less than full length samples on Q and η should be mentioned. Although no quantitative results were obtained, it seems reasonable for $(L-L')/L \lesssim \frac{1}{4}$ that Q should not greatly decrease and might even increase since the microwave fields will be weaker near the end walls. A decrease in η is expected because of less filling, but it would seem that this decrease would be small since most of the contribution to the sample filling integral occurs near the center of the cavity.

ACKNOWLEDGMENTS

The authors wish to acknowledge the technical assistance of J. Dennis, D. Heatherly, S. Pan, and W. Snow, Jr.

*Research was supported by the Air Force Office of Scientific Research, Air Force Systems Command.

†Present address: Astronomy Department, Cornell University, Ithaca, New York 14850.

‡Present address: Physics Department, University of Michigan, Ann Arbor, Michigan 48104.

[1]R. S. Alger, *Electron Paramagnetic Resonance* (Wiley, New York, 1968). This text provides outstanding background material from a practical point of view and, in addition, provides necessary references to the original literature.

[2]Z. Haniotis and G. H. Gunthard, Z. Angew. Math. Phys. **20,** 771 (1969).

[3]These are equivalent to those found in *Techniques of Microwave Measurement*, edited by C. G. Montgomery (McGraw-Hill, New York, 1947).

[4]G. Feher, Bell Syst. Tech. J. **36,** 449 (1957).

[5]J. S. Hyde, Varian Assoc. Tech. Inf. Bull. Fall, 10 (1965).

[6]Stycast is a low loss dielectric material whose dielectric constant can be controlled by the manufacturer, Emerson and Cuming, Inc., Canton, Massachusetts 02021.

[7]*Dielectric Materials Supplement Chart* (1966). Obtained from Emerson and Cuming, Inc., Canton, Massachusetts 02021.

[8]*Brochure A2005* (1969). Obtained from Carborundum Co., P. O. Box 311, Latrobe, Pennsylvania 15650.

[9]*Preliminary Technical Bulletin 7-2-2A,* Emerson and Cuming, Inc., Massachusetts 02021.